Geochimica et Cosmochimica Acta Vol. 53, pp. 1717–1726

0016-7037/89/$3.00 + .00

Introduction to the hydrogeochemical investigations within the International Stripa Project*

DARRELL KIRK NORDSTROM[1], TOMMY OLSSON[2], LEIF CARLSSON[3] and PETER FRITZ[4]
[1]U.S. Geological Survey, 345 Middlefield Road, Menlo Park, CA, 94025, U.S.A.
[2]Geosystem AB, Box 8020, S-75008 Uppsala, Sweden
[3]Swedish Geological AB, Kungsgatan 4, S-4119 Göteborg, Sweden
[4]Institut für Radiohydrometrie, Gesellschaft für Strahlen und Umweltforschung, D-8042 Neuherberg, F.R. Germany

(Received April 8, 1988; accepted in revised form April 26, 1989)

Abstract—The International Stripa Project (1980–1990) has sponsored hydrogeochemical investigations at several subsurface drillholes in the granitic portion of an abandoned iron ore mine, central Sweden. The purpose has been to advance our understanding of geochemical processes in crystalline bedrock that may affect the safety assessment of high-level radioactive waste repositories. More than a dozen investigators have collected close to a thousand water and gas samples for chemical and isotopic analyses to develop concepts for the behavior of solutes in a granitic repository environment. The Stripa granite is highly radioactive and has provided an exceptional opportunity to study the behavior of natural radionuclides, especially subsurface production. Extensive microfracturing, low permeability with isolated fracture zones of high permeability, unusual water chemistry, and a typical granitic mineral assemblage with thin veins and fracture coatings of calcite, chlorite, sericite, epidote and quartz characterize the site. Preliminary groundwater flow modeling indicates that the mine has perturbed the flow environment to a depth of about 3 km and may have induced deep groundwaters to flow into the mine.

INTRODUCTION

REPORTS OF DEEP SALINE groundwaters from crystalline rocks have been published for over one hundred years, mostly from the mining industry. Geochemical research on deep crystalline rock aquifers, however, has been sparse until the last ten years. New and unusual chemical and isotopic data have led to the advancement of several hypotheses to explain the occurrence of brackish to saline groundwaters and even brines up to 325 g/L (total dissolved solids) in the Canadian Shield, the Fennoscandian Shield and the Ukrainian Platform (see, *e.g.*, FRITZ and FRAPE, 1987). Much of this research has been motivated by the need to find a safe disposal for high-level radioactive waste and by the concept that crystalline, usually granitic, bedrock is highly impermeable, non-reactive and has considerable mechanical and thermal integrity. The Stripa Project is one such project that has brought together an international group of geochemical and isotopic specialists to investigate the origin and evolution of groundwaters in a small granitic intrusion in Central Sweden. An abandoned iron ore mine provided the opportunity for subsurface drilling and sampling.

The first twelve articles of this issue describe the research results from the Hydrogeochemical Advisory Group (HAG) and their associates of the International Stripa Project. This project began as a Swedish-American Cooperative (SAC) Program in 1977 jointly carried out by Lawrence Berkeley Laboratory (under sponsorship of the Department of Energy) and the Division KBS of the Swedish Nuclear Fuel Supply Company (now known as the Swedish Nuclear Fuel and Waste Management Company, SKB or Svensk Kärnbränslehantering AB). The original objective of the program was to investigate the thermal and mechanical properties of granite; later, it was expanded to develop and evaluate techniques for measuring the thermomechanical, hydrogeological, geophysical and geochemical properties and processes necessary to assess the conditions for the safe disposal of high-level radioactive waste in granitic bedrock. The abandonment of the Stripa iron ore mine in central Sweden provided the opportunity to establish a research site for these purposes. The site will never be used as a repository, only to carry out basic research.

In May, 1980, the International Stripa Project was formed from the original SAC Program, and it has boasted the participation of nine countries: Canada, Finland, France, Japan, Spain, Sweden, Switzerland, the United Kingdom, and the United States. The project is coordinated by OECD/NEA and managed by SKB. Three phases of research have been defined: Phase I for the period 1980–1984, Phase II for the period 1984–1986 and Phase III for the period 1986–1990. Phase I activities have included hydrogeological testing in boreholes, tracer migration experiments, hydrogeochemical investigations of groundwaters, geophysical detection and characterization of fracture zones and field investigations on the behavior of bentonite clay as backfill and sealing material. The following hydrogeochemical papers are based on the hydrogeochemical activities from the SAC Program, Phase I, and some of the recent Phase II results. Although hydrogeochemical activities during Phase III are not anticipated at this time, further investigations are still being completed in an extended program of Phase II.

The intent of this paper is to provide a summary of the hydrogeological background of the Stripa site, including the main hydrologic and geologic properties and to introduce the following papers in this issue. The next paper describes the main characteristics of the groundwater chemistry, along with a discussion of water-rock interactions likely to control these characteristics. The third paper presents the results of fluid-inclusion determinations and the possible role of fluid inclusions in contributing solutes to the groundwater. The next three papers primarily cover stable isotope determinations on the water, dissolved sulfate, dissolved carbonate and calcites as a means of interpreting the source of the groundwater and its solutes. Included are discussions of tritium and carbon-14 data. Following these stable isotope papers, there is a paper dealing with the calcite fracture mineralogy with strontium

* This paper is published as part of a series reporting results of the International Stripa Project.

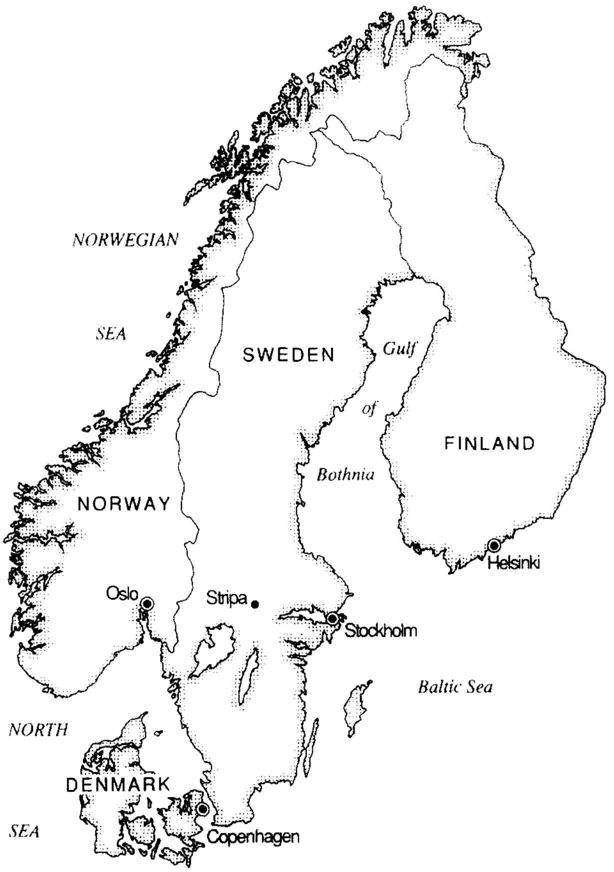

FIG. 1. Location of the Stripa research site in central Sweden.

isotope data. Some strontium isotope results from the fracture minerals and groundwaters have already been published by B. FRITZ *et al.* (1987). The last five papers deal with investigations on the radioisotopes and gases found in both rock and groundwater at Stripa. These last papers reflect a considerable effort in detailing processes that may affect radionuclide behavior in a granite that has a radioactivity much greater than the average granite. Special attention has been paid to the subsurface production of radionuclides and mechanisms of their mobility. Overall, these papers exhibit a range of chemical and isotopic investigations that has rarely been paralleled by any other program. These investigations also were the first of their type ever to be carried out in the Fennoscandian Precambrian Shield.

The field investigations were carried out at the Stripa mine, located in southern central Sweden (59°43'N, 15°5'30"E), 250 km west-northwest of Stockholm (*cf.* Fig. 1). The mine is located within the Central Swedish Ore Province comprising more than a hundred iron-manganese and copper-zinc-lead mines. Mining at Stripa began around the year 1450 for iron. The mining was intermittent but continued until 1976 after which the mine was kept open only for research.

Boreholes at two selected sites in the Stripa mine have been used for different hydraulic measurements and to collect the required water and rock samples for the hydrogeological and hydrogeochemical program. These sites are located at 360 m and 410 m below the ground surface. The main site, at 360 m level, has three boreholes, one vertical borehole 505 m deep (V1), and two 300 m long subhorizontal holes (N1 and E1). This site is located at the eastern-most tip of the mined areas and well within the granite. A fourth borehole (V2) is located at the 410 m level and is a deepening of an old borehole (Dbh1) to a present depth of 822 m (1232 m below the ground surface). The location of the test sites and the boreholes are shown in Fig. 2. In addition to these boreholes, a number of other boreholes have also been used for minor sampling and testing.

It should be noted that it was never the main objective of the Stripa Project to characterize the geology and hydrology of the site and its environs. Consequently, some of the geologic and hydrogeologic characteristics of the research site are not known.

GEOLOGY

Petrology

The rock type for all investigations in the Stripa Project is a rather small intrusive body of granite—the Stripa granite, which is predominantly a grey to reddish, medium-grained granite of Precambrian age. WOLLENBERG *et al.* (1980) estimated the age at 1.69 Ga by K-Ar dating and B. FRITZ *et al.* (1987) estimated a minimum age at 1.71 Ga by Rb-Sr dating. The Stripa granite occurs at the surface in a belt of older supracrustal rocks with structures striking mainly NE-SW (*cf.* KOARK and LUNDSTRÖM, 1979). Post-emplacement cooling produced fracture coatings dated at 1.63 Ga by Rb-Sr dating (B. FRITZ *et al.* 1987). The main geologic features of the site are shown in Fig. 3.

The matrix of the granite consists of approximately 35% by volume of quartz, 30% of partly sericitised plagioclase, 25% of K-feldspar, 5% of muscovite and 3% of chlorite. Accessory minerals (carbonates, epidote, fluorite, zircon, garnet, apatite and magnetite) are typically <1% (WOLLENBERG *et al.*, 1980; R. J. DONAHOE, pers. commun.).

Leptite, a strongly metamorphosed sedimentary rock of volcanic origin, is the dominant rock type in the supracrustal formation. The iron ore previously mined at Stripa is associated with the leptite formation (see Fig. 3). The leptite is mineralogically similar to the granite. Texturally, however,

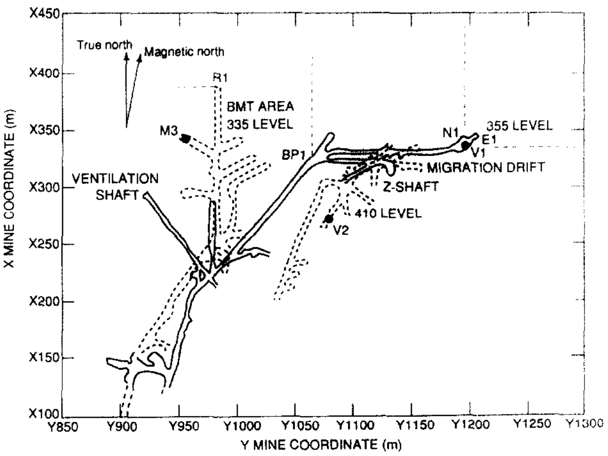

FIG. 2. Location of the underground adits and drillholes at Stripa.

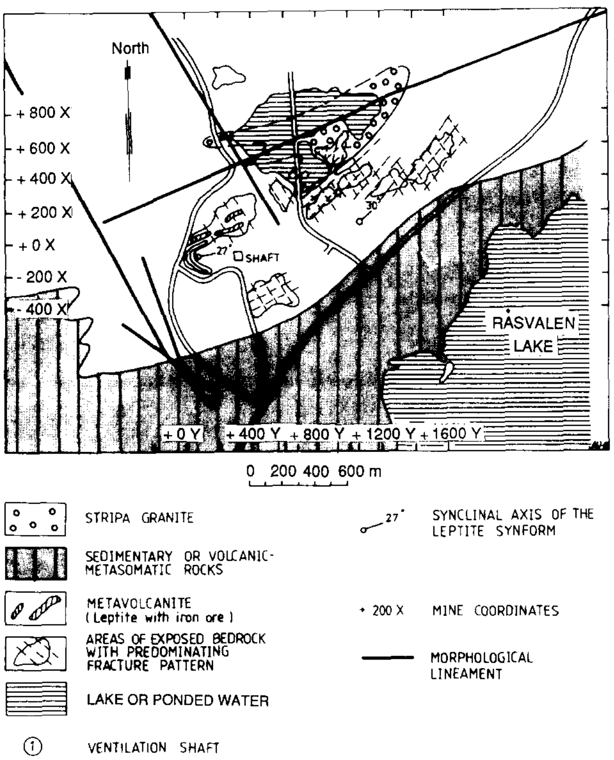

FIG. 3. Major geologic structures in the Stripa area.

it does not resemble the granite, it is finer, more even-grained and homogeneous.

The ore deposit associated with the leptite is recognized mainly as two bodies, one main body and a smaller body parallel to the main. The main body has a maximum thickness of 16–17 m and is folded into a syncline with an undulating eastward pitch. The iron ore is mainly a quartz-banded hematite, but magnetite occurs also. The skarn minerals associated with the ore are actinolite, diopside and epidote. Pyrite occurs locally and is evidently of secondary origin (GEIJER, 1938). The ore in the main body has a higher content of Fe than the ore in the parallel body. The main body contains 50% Fe, 0.007% P and 0.016% S and the parallel body contains 41% Fe, 0.009% P and 0.037% S (PAULSRYD, 1941).

Chemistry of the Stripa granite

Seven samples of the Stripa granite have been analyzed (all in duplicate) by X-ray fluorescence, emission spectroscopy and ion-selective electrodes. Four of these samples were taken from borehole V1 at depths of 107, 408 and 445 m in the borehole and three were taken from borehole V2 at depths of 456, 471 and 760 m. The results of the analyses are reported in Table 1. They are in excellent agreement with a more limited data set reported by WOLLENBERG *et al.* (1980). Based on the chemical data given in Table 1 the Stripa granite can be classified as a peraluminous granite by the criteria $Al_2O_3 > Na_2O + K_2O + CaO$ (BARKER, 1981).

Rare earth elements plus Ba, Co, Cr, Cs, Hf, Rb, Sb, Ta, Th, U, Zn, Zr and Sc have been determined on 14 granite samples by NAA at the U.S. Geological Survey. These results are shown in Table 2. These data were necessary for calculations of *in situ* production of radionuclides.

Fracture minerals

All boreholes within the program show similar characteristics regarding the existing fractures. Detailed fracture logs are given in Stripa internal reports on the core logs (CARLSSON *et al.*, 1981, 1982a,b). The recorded fractures may be classified into one of five different groups:

1. Fractures with fresh, uneven surfaces;
2. Open or sealed fractures;
3. Small-scale shear zones;
4. Brecciation and granulation of the granitic matrix;
5. Quartz veins.

Except for the fractures included in the first group, all others are characterized by the existence of mineral coatings on the fracture surfaces. The fracture-fill minerals have been mega-

Table 1. Chemical analysis of seven stripa granite samples.

		V2-456	V2-471	V2-760	V1-107	V1-408	V1-408.03	V1-445	Average
SiO_2	%	76.3	76.9	76.3	75.9	76.6	78.1	77.5	76.8±.75
Al_2O_3	%	14.0	13.7	14.0	14.0	13.9	14.0	14.2	14.0±.21
Fe_2O_3	%	1.5	1.2	1.4	1.2	1.2	1.4	1.4	1.33±.18
MgO	%	.24	.26	.25	.26	.24	.28	.30	.26±.02
CaO	%	1.0	.72	.87	.80	.40	.43	.76	.72±.22
Na_2O	%	4.1	3.9	4.0	4.0	4.0	4.0	4.4	4.07±.22
K_2O	%	4.9	5.0	4.6	4.6	4.6	4.7	4.1	4.62±.29
TiO_2	%	.08	.08	.09	.08	.09	.08	.09	.08±.01
P_2O_5	%	.09	.09	.09	.08	.09	.10	.10	.09±.01
MnO	%	.05	.05	.05	.07	.05	.05	.06	.06±.01
Cl	%	.018	.013	.018	.015	.012	.020	.018	.016±.004
F	%	.052	.074	.061	.056	.019	.023	.024	.044±.021
S (total)	%	.03	.02	<.01	<.01	<.01	<.01	<.01	≤.03
Li (ppm)		1.8	2.8	28	8.4	4.5	4.6	5.5	7.9±8.7
B (ppm)		3	3	3.5	5	4	4	4	3.8±0.9

Analysts: J. Gillison, N. Rait, J. Fletcher, R. Johnson (U.S.G.S.). Results from 7 samples done in duplicate. Averages are for 14 determinations of each constituent with one standard deviation. Note that rock samples are from clean, unfractured sections of core, and the analyses represent fresh granite. Higher concentrations of some constituents will be encountered in highly fractured rocks, especially where fracture-fill minerals occur.

Table 2. NAA Analyses of Stripa Granite.

Element (ppm)	V2-456	V2-471	V2-760	V1-107	V1-408	V1-408.03	V1-445	Average
Ba	511	659	571	513	474	525	565	545±60
Co	0.67	0.64	0.76	0.71	0.64	0.73	0.81	0.71±0.06
Cr	<1	1.8	1.0	1.6	1.2	2.7	1.7	1.7±0.6
Cs	4.3	4.3	9.1	3.1	2.6	3.1	3.4	4.3±2.2
Hf	3.7	3.7	4.0	3.7	3.8	3.8	3.9	3.8±0.12
Rb	261	307	282	271	245	249	265	269±21
Sb	0.17	0.13	0.23	0.27	0.12	0.17	0.22	0.19±.05
Ta	7.9	8.0	6.8	8.8	7.8	7.9	7.8	7.9±0.6
Th	31	31	36	32	34	34	34	33±1.9
U	31	33	35	32	26	31	33	32±2.8
Zn	19	11	22	23	16	21	19	19±4.1
Sc	4.5	4.5	5.5	4.4	4.7	5.2	4.9	4.8±0.4
La	27	26	31	26	28	29	32	28±2.4
Ce	70	66	80	67	73	75	80	73±5.7
Nd	35	35	42	33	36	39	44	38±4.1
Sm	7.8	7.4	9.1	7.6	8.4	9.1	9.4	8.4±0.8
Eu	0.45	0.41	0.50	0.42	0.44	0.46	0.47	0.45±0.03
Gd	13	13	14	13	12	14	15	13±1.0
Tb	2.1	2.1	2.4	2.1	2.1	2.3	2.3	2.2±0.13
Tm	1.1	1.0	1.0	1.0	1.0	1.0	1.2	1.0±0.08
Yb	8.0	8.2	9.1	8.1	8.3	8.8	8.6	8.4±0.4
Lu	1.2	1.2	1.4	1.2	1.2	1.2	1.3	1.2±0.08

scopically classified on the basis of color, hardness and presence of carbonates. Different fracture-fill minerals are intergrown in varying combinations which makes a megascopical classification somewhat uncertain. An extra check has therefore been made by using X-ray diffraction on five samples taken from the V2 core. The result showed that the plagioclase intergrown with epidote was much more common than expected. The conclusion which may be drawn from the result is that plagioclase content in general has been underestimated.

Chlorite, which is the most common fracture mineral, is very dark, almost black, and much harder than normal due to intergrowths of epidote and plagioclase. Sericite, commonly intergrown with chlorite, is nearly as common as chlorite.

Next to chlorite and sericite, calcite is the most common fracture mineral. Its occurrence ranges from fillings of hairline cracks and thin coatings and intergrowths with other minerals to coarse crystals grown in the spacings of large fractures.

Epidote occurs commonly in sealed fractures, veins and shear zones and associated with quartz, chlorite and sericite. The epidote shows many types of color variations in the green spectrum when occurring with plagioclase. Other fracture-fill minerals identified in the cores include pyrite, chalcopyrite, fluorite, iron oxides and zinc sulfide. The great majority of the fracture infillings are less than 1 mm in width.

Borehole V2 penetrates the most deep-seated rock mass and it was therefore of interest to study the variation in mineral coatings *versus* depth. The result of this study is summarized in Fig. 4, where it is seen that the coatings of chlorite and chlorite/calcite are about constant throughout the full length of the borehole. Chlorite, calcite and epidote make up about 25–30 percent of all coated surfaces. Pyrite, fluorite, iron oxides, zinc sulfide and clay minerals make up the remaining percentage. The most striking change with depth is that the calcite shows a marked decrease at 250–450 m depth with a simultaneous increase in epidote. These observations are generally in agreement with the results reported by WOLLENBERG *et al.* (1980), which is based on visual identification, X-ray diffraction analyses and analyses of thin sections. An additional observation is the rare but noteworthy occurrence of asphaltite as fracture fill in the Stripa granite (WOLLENBERG *et al.*, 1980). Nothing is known about the origin of this organic material and it was found to contain high concentrations of uranium.

Additional studies of fracture minerals have been reported by P. FRITZ *et al.* (1980). Chalcopyrite was found in one sample and some analyses of muscovite, sericite, Ca-mica, chlorite, feldspar, pyrite and calcite are reported. The compositional data for chlorite indicate that there are two varieties: an iron-rich member (FeO/MgO = 7) and a magnesium-rich member (FeO/MgO = 0.9). This observation is consistent with the optical information on chlorites in the rock matrix that indicates two species of different composition. More recent studies by B. FRITZ *et al.* (1987) indicate the majority of fracture coatings are associated with late stage hydrothermal activity during the final cooling of the pluton (late Proterozoic in age). Some recrystallization of these coatings no doubt

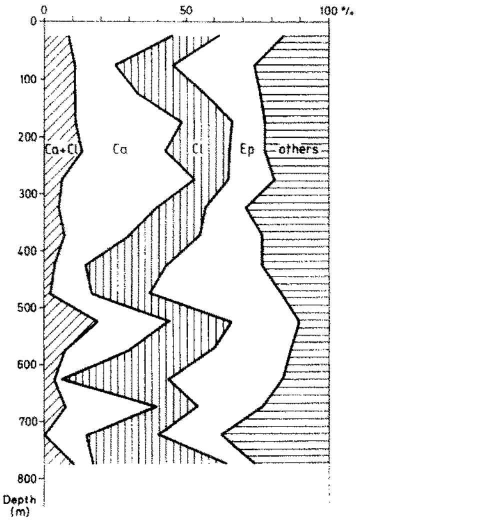

FIG. 4. Distribution of the fracture-fill minerals in borehole V2 with depth by volume: Ca = calcite, Cl = chlorite and Ep = epidote.

Table 3. Radioelement contents (after Wollenberg et al., 1980).

Rock Type	No.	Uranium ppm	Thorium ppm	Potassium %	Th/U
Stripa Granite					
Surface	9	26.9±5.5	33.0±5.7	4.6±0.7	1.1±0.1
Underground	34	37.4±6.2	29.2±3.8	3.9±0.3	0.8±0.1
Leptite					
Surface	5	3.3±0.7	11.9±2.9	3.1±0.6	3.6±0.4
Underground	9	5.4±3.1	17.9±1.4	2.8±0.5	3.9±1.2
Regional Rocks					
Granites	7	17.6±15.4	26.6±6.6	5.2±1.5	2.4±1.2
Metamorphic	5	6.1±1.5	14.6±8.7	2.5±1.1	2.6±1.9

Table 4. Radiogenic heat production of the rock in the Stripa Region (Wollenberg et al., 1980).

Rock Type	No.	Heat Production μW/m³
Stripa Granite		
Surface	9	9.5
Underground	34	11.9
Leptite		
Surface	5	2.0
Underground	9	2.9
Regional Rocks		
Granites	7	6.8 to 7.1
Metamorphic	5	2.8

took place during the Phanerozoic but the evidence for it is very difficult to find and challenging to interpret.

Radiogeology

The abundance of radioelements in the rock has been measured by WOLLENBERG *et al.* (1980). The fission-track radiographic method was used to determine the location and abundance of uranium in uncovered thin sections.

The Stripa granite is rather unique in its radioelement content, both in the abundance of elements and their ratios. Table 3 indicates the relatively high uranium and thorium contents of the granite, compared with other plutons in the region.

The measurements indicate that uranium is depleted in surface exposures of granite and leptite at Stripa, relative to its abundances in the same rock units underground.

In the Stripa granite, uranium is highly concentrated in tiny opaque grains on the order of 50 micrometers in diameter, generally euhedral and in some places square in cross-section. These grains are usually found in chlorite, but also in muscovite-chlorite-sericite filled fractures, and even in cracks within quartz or feldspar. Usually the grains contain up to 5% uranium, but concentrations up to 10–15% have been observed (WOLLENBERG *et al.*, 1980). Another locus of uranium concentration was observed in opaque grains with both a quartz-epidote-sericite-filled fracture on a contact between granite and leptite, and with fine carbonate-sericite stringers intersecting that contact on the granite side. Although the concentration of uranium is lower in these grains, on the order of 2% U, the absolute abundance of uranium contained in them is greater.

Uranium is also found, in lower concentrations, dispersed along chlorite-filled fractures without associated discrete grains. Concentrations are generally about 0.5% or lower, but occasionally range up to 1.0% uranium. The Stripa leptite contains no appreciable discrete concentration of uranium either in the matrix or in a coarse epidote-filled fracture cutting it (WOLLENBERG *et al.*, 1980). Uranium minerals were observed in chlorite-filled fractures cutting the iron ore at Stripa (WELIN, 1964).

The heat production from the radioelements of the Stripa pluton has been calculated by WOLLENBERG *et al.* (1980). These values are compared to those for other rocks in the region in Table 4. The Stripa granite has about four times the radiogenic heat production of the "average" granite (taken as 2.8 microwatts/m³ from HEIER and ROGERS, 1963) and nearly twice the production of other granites in the region.

Geophysical well logs have played an important part in the current program to determine hydraulic, structural, stability and chemical parameters in the drillholes. A standard geophysical well-logging program was set up and performed in the four main boreholes. In this respect, the results of natural gamma logs are of interest and the results in terms of radiation are presented in Table 5. The high level in borehole N1 is due to high radon content in combination with the very low water outflow. The radiation level in the granite is most accurately given by values from V1 where the water outflow is high and thus no enrichment of radon in the water.

Structure

Figure 3 shows the major structures in the Stripa area. The lineaments in the granite have a direction generally parallel to the syncline axis of the supracrustal formation.

The fractures decrease in frequency with increased depth as shown in Fig. 5. Near the ground surface the fracture frequency is between 3 and 5 fractures per m, while at depths of 1000 m and below it is well below 1 fracture per m. In addition to the discrete fracturing, a number of fractured zones cut through the granite. These zones are normally of limited extension and hydraulic significance. However, one major structure, a large fracture zone of crushed rock, was located in one of the boreholes (V1) at a depth of about 800 m. This zone is of great significance to the hydraulic properties in the area and to the groundwater chemistry as it conducts water rapidly to great depths as evidenced by the presence of tritium.

A detailed compilation of fracturing has been impractical for the strongly crushed part of the V1 borehole (466 m down

Table 5. Radiation level in the boreholes E1, N1, V1 and V2.

BH	Average	Peak
V1	65 μR/h	406 μR/h
V2	100 μR/h	250 μR/h
E1	117 μR/h	
N1	250 μR/h	430 μR/h

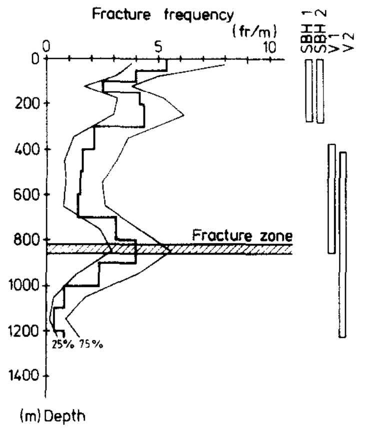

FIG. 5. Fracture frequency with depth based on data from boreholes SBH1 (shallow borehole 1), SBH2 (shallow borehole 2), V1 (vertical borehole 1) and V2 (vertical borehole 2).

to the bottom of the borehole at 505 m). Totally 7.7 m of this section is disconnected or crushed to rubble. The fracture frequency was 12.9 fr/m in the zone to be compared to 1.5 fr/m for the rock mass above the zone.

Figure 6 shows a cumulative fracture diagram for borehole V2 with regard to the dip of the fractures. It is seen that medium steep fractures of 31–61° dominate while steeply dipping fractures have a low frequency. Flat-lying fractures are intermediate in frequency. This is in full agreement with the result obtained in borehole V1 (CARLSSON, *et al.*, 1981). It must be stressed that the vertical borehole V2 tends to underestimate vertical or steeply dipping fractures while sub-horizontal or flat-lying fractures are recorded with their actual frequency. The flat-lying fractures show a low frequency below approximately 400 m depth with 0.3 fr/m which decreases down to 0.1 fr/m in the lowermost 230 m. This condition indicates that medium steep or steep fractures might dominate the fracture system at depth and horizontal fracturing becomes more sparse. This suggestion is supported by the data from horizontal boreholes.

The fracture pattern which predominates in the rock mass at the main borehole site (360 m level) are steeply dipping fractures in N30E based on horizontal boreholes N1 and E1. Other fracture sets of importance are N30W and N10E, both steeply dipping. Comparing both vertical and horizontal borehole data, the steep fractures clearly dominate the fracture pattern and make up as much as 40 percent of all fractures in the rock mass adjacent to the test site. Medium steep fractures make up 31 percent and the remaining 20 percent are attributed to flat-laying fractures. The existing fracture sets are shown in the semispherical projection in Fig. 7.

HYDROGEOLOGY

Hydraulic units

The hydraulic properties of a crystalline rock mass such as the Stripa granite are characterized by fractures, faults and other discontinuities which transect the rock. The granitic rock matrix is, from a practical point of view, almost impervious and the main flow paths are constituted by the fracture system, zone of fractured or crushed rock and other structural discontinuities. As shown above, there exist a number of discontinuities, some of which are associated with the synclinal structure of the sedimentary sequence and others more independent of it. The dominant deformation took place before or during the intrusion of the pluton and the granite is intersected only by a few large fracture zones, although it is highly fractured on a small scale.

The dominant ruptural deformation is concentrated in the superficial part of the rock, which shows a rather high fracture frequency and a high hydraulic conductivity. This more frac-

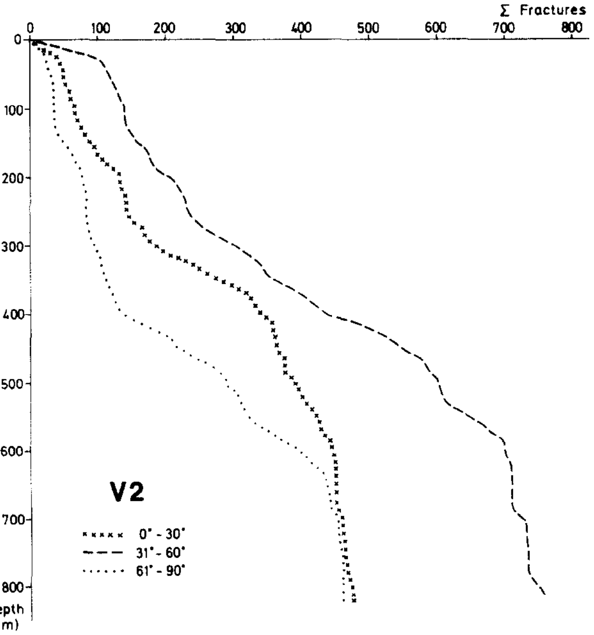

FIG. 6. Cumulative fracture diagram for borehole V2.

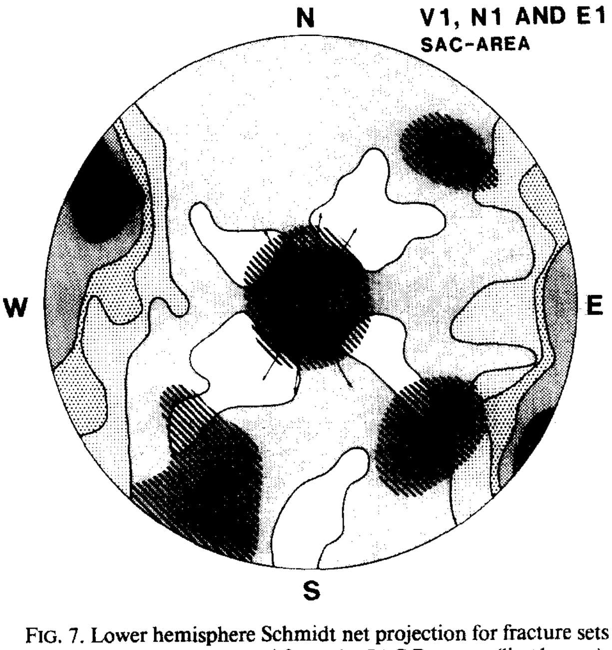

FIG. 7. Lower hemisphere Schmidt net projection for fracture sets obtained from V1, N1, E1 and from the SAC Program (lined areas).

tured part of the rock mass extends down to about 250 m depth. Below this level the rock becomes more sparsely fractured, with fractures which are sealed to a great extent. The fracturing continues to decrease and reaches its lowest frequency below the 1,100 m level (*cf.* Fig. 6). In the deep-seated rock mass the water flow seems to be channeled in relatively few zones of fractured rock, where the permeable fracture zone found in the lowermost part of V1 is an extreme example of these flow paths.

The mine itself is one of the most important structures governing the water flow in the area. It acts as a drainage center in which the water table has been successively lowered as the mining continued. During the SAC-program, efforts were put into characterizing the draining effect of the mine. As reported by GALE (1982), piezometric recordings taken at different levels in boreholes SBH-1, SBH-2, SBH-3 and V2 showed that there is a downward gradient above the excavations. Around the test areas, the groundwater gradients are directed towards the excavations.

Porosity of the rock mass

According to NORTON and KNAPP (1977) the total porosity in a fractured medium, Θ_T, may be expressed as

$$\Theta_T = \Theta_K + \Theta_D + \Theta_R$$

where

Θ_K = effective flow porosity or kinematic porosity
Θ_D = diffusion porosity
Θ_R = residual porosity.

The kinematic porosity represents the fractures through which the dominant fluid flow proceeds, while the diffusion and residual porosities refer to fractures or pores in which no or very limited flow occurs. The fractures making up the residual porosity are not connected with those included in either the kinematic or the diffusion porosity. Figure 8 illustrates the geometric relationship between the different porosities.

Calculations of the porosity based on hydraulic measurements in drill-holes will result in different porosity values depending on the penetration of the drill-hole in different fracture sets. Moreover, the existing joint sets have different properties, a point discussed by PARSON (1972) and CARLSSON (1979).

The rock matrix has a very low hydraulic conductivity where the normal fractures connected only over a shorter distance constitute the majority of flow paths. The conductivity is estimated to be in the range 10^{-13}–10^{-16} m/s, depending on the degree of fracturing. Although the conductivity is low, the storativity is fairly high, the average total porosity according to resistivity logs is 0.47%. Porosity measurements were made on 12 samples from N1 and 6 samples from V1. The results are very consistent, with a minimum value of 0.36% and a maximum of 0.61%. GALE *et al.* (1987) have estimated porosities in the Stripa granite from steady-state flow tests (outflow and injection tests) in the field, hydraulic lab tests, aperture measurements and injected resin thicknesses. They found the hydraulic tests and the resin thicknesses were roughly comparable in porosity results (0.06–0.26%), whereas the field data were about two orders of magnitude less (0.0015–0.0041%). These porosity values are all biased and cannot adequately estimate the total porosity due to the testing procedure. The actual total porosity may be 50–200% higher. Measurements of fluid inclusion populations (see NORDSTROM *et al.*, 1989, this issue), indicate 1–2% residual porosity, the largest component of the total porosity.

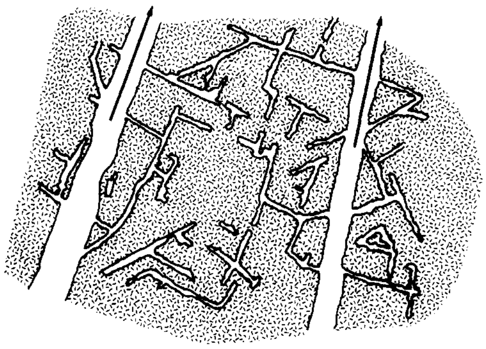

FIG. 8. Schematic representation of the three types of porosities: kinematic (shown by arrows indicating arbitrary flow direction), diffusion (smaller pores connected to kinematic fracture openings) and residual (closed pores) based on NORTON and KNAPP (1977).

Most of the pores and fractures included in the total porosity are not actively contributing to the flow porosity. The flow porosity is estimated to be in order 10^{-5}–10^{-4} which is only 2–20 permille or less of the total porosity (CARLSSON and OLSSON, 1985). However, in the heavily fractured part of V1, the flow porosity is higher and estimated from hydraulic tests to be in the range $1–5 \cdot 10^{-4}$.

Hydraulic conductivity of the rock mass

A naturally fractured formation is generally represented by a tight matrix broken up by fractures of secondary origin. The fractures vary considerably in size from voids and interconnected channels to fine cracks. Some of the fractures are assumed to be continuous throughout the formation and to represent the paths of principal hydraulic conductivity. The rock matrix, consisting of poorly connected microcracks and closed micropores, has a lower hydraulic conductivity but generally a higher primary porosity.

The groundwater system at the Stripa Mine has progressively been affected by the mining activities. As the mine was sunk, new flow paths were activated and the water table was successively lowered. The groundwater system has almost continuously adjusted to the drainage from the underground drifts, *i.e.* the groundwater system has been in a steady-state condition. In 1976 the mining was terminated, but the drainage pumping continued. This has given a hydraulic situation which is well suited for hydrogeological studies underground, as any controlled disturbance due to testing should take place in a steady-state groundwater system.

A number of techniques may be applied to the underground hydraulic testing. However, requirements and demands from other activities and research programs make some of the possible techniques less suitable. In order to obtain accurate water sampling and analytical results, the groundwater system should be contaminated as little as possible with external water and other chemical compounds. This condition calls for testing techniques where the groundwater should be extracted rather than injected. Other test programs within the Stripa Project, as for instance, the Buffer Mass Test (engineering tests on backfill), are strongly dependent on an undisturbed supply of groundwater and pressure build-up, which calls for minor extraction and disturbance on the water head around the mine.

However, as the hydraulic testing takes place deep underground, in the potential sink made up by the mine, it was found convenient to utilize the existing potential field for the testing, *i.e.* to use the natural drainage for water extraction as the main tool and to measure the pressure build-up after shut in and the fall-off after release. By this technique, no foreign water is introduced into the groundwater system, and the overall disturbances on the head should be negligible. This technique was used as the main tool both in single hole tests and in hydraulic interference tests. However, limited water injection tests were also carried out in order to compare the results from different techniques.

Three different interference tests were also conducted during the program, *i.e.*: (1) interference tests between the boreholes V1 and V2; (2) interference tests between the boreholes V1, V2, N1 and E1; (3) interference tests between the borehole N1 and the BMT-area. In each of these, a specific test section in one of the boreholes was packed off and pressurized. Sections of other boreholes were packed off and resulting pressure change was recorded.

The interference tests made in the mine show that there is a clear hydraulic interconnection between boreholes V1 and V2 and between N1 and BMT-area. On the other hand, it is also clear that no interconnection was obtained between V2 and N1 or between E1 and N1. A slight influence was noted between the fractured zone in V1 and the innermost part of N1.

The great number of hydraulic tests have produced values on the hydraulic conductivity of the Stripa granite. Tests exist for the surface boreholes as well as from subsurface holes in different test sites, from the large scale ventilation test and from the large scale injection test. This huge stock of values provides a good base for determinations of the water flow in the granitic rock mass around the mine. Table 6 summarizes the range in conductivity results from the SAC-program and the present program.

The conductivity is at its maximum in surface boreholes, about $5 \cdot 10^{-8}$ m/s, while it is $1 \cdot 10^{-9}$ m/s or lower in the tests made down in the mine. The large scale ventilation and injection tests, which both are measures of the gross conductivity, gave low values of $1 \cdot 10^{-11}$ m/s and $4 \cdot 10^{-11}$ m/s, respectively. Those latter values are probably representative for the rock mass including minor zones of fractured rock.

Table 6. Hydraulic conductivity data of the Stripa granite obtained during the SAC Program and the current program.

Test Type	Conductivity Range m/s	Ref
Injection Surface Holes	5 x 10^{-11} - 5 x 10^{-8}	1
Injection Ventilation Drift	1 x 10^{-12} - 1 x 10^{-9}	1
Ventilation Test	1 x 10^{-11}	2
Large Scale Injection	4 x 10^{-11}	3
V1, Fracture Zone	1 x 10^{-7}	4
V2, Rock Mass	2 x 10^{-12} - 2 x 10^{-8}	4
E1	4 x 10^{-12} - 4 x 10^{-8}	4
N1	6 x 10^{-13} - 4 x 10^{-8}	4

1. Gale (1982); 2. Witherspoon et al. (1980); 3. Lundström and Stille (1978); 4. Carlsson and Olsson (1985).

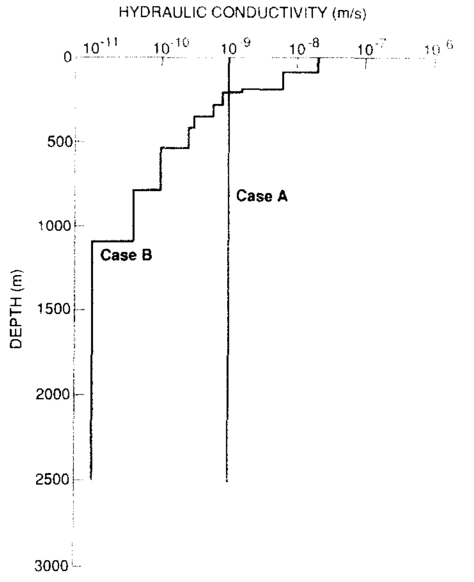

FIG. 9. Hydraulic conductivity *versus* depth used in model calculations.

Two zones have been found with relatively high conductivity, one 40 m wide zone in V1 (40 m along the borehole) with a conductivity of $7 \cdot 10^{-8}$ m/s and one 2 m wide zone in E1 with $4 \cdot 10^{-8}$ m/s. Besides these zones, the obtained conductivity is lower than 10^{-9} m/s with 10^{-13} m/s as the lowest recorded value. This is also the lower limit for the techniques and the equipment used.

Model calculations

Preliminary calculations have been made of the groundwater inflow to the mine. The calculations were based on available data on hydraulic conductivity and topographical conditions. The calculations were performed for a vertical plane laid out from the center of Lake Rosvalen, through the mine and further on about 4 km towards NNW. In total, the section was 7 km in length and 2.6 km in depth. The mine was illustrated as two horizontal drifts, each 1,000 m in length at the levels 410 m and 290 m, respectively. The height of the drifts was taken as 70 m.

The calculations were carried out using a finite-element program and assuming two-dimensional flow at steady state. The lower and vertical boundaries of the studied plane were set as no-flow boundaries. The groundwater head at the upper boundary was given as the ground-surface. At the mine the head was set as the datum level. Results of the calculations give the head distribution around the mine together with the inflow to the mine.

The hydraulic conductivity of the rock mass was given different values to illustrate different possible conditions in the rock. The conductivity distribution *versus* depth is given in Fig. 9. The results of the calculation given as distance of influence on the head and the water inflow are summarized in Table 7.

Table 7. Results of Finite Element Calculations of the Distance of Influence and the Groundwater Inflow.

Assumptions made for conductivity distribution		Horizontal distance for 50 m influence at mine level (km)	Water inflow to the mine (l/min)
Case A.	Constant conductivity	0.8	73
Case B.	Exp. decreasing conductivity with depth	0.45	96

The actual inflow to the mine for period January 1983–September 1984 was recorded to be about 470 l/min on the average.

The result from the calculations based on decreasing conductivity values *versus* depth (Case B) is more realistic as it is based on actual test results from the area. The groundwater head for this distribution is given in Fig. 10, where the impact of the mine is clearly visualized.

It should be noted that the calculated inflow value does not specify flow in discrete fractured zones. These zones, as the one in borehole V1, are probably the cause for the major part of the actual inflow to the mine.

Regional flow pattern

It is also worthwhile to examine the regional flow pattern as it defines the residence time in different rock types for different groundwaters at different depths. An attempt to define this flow pattern has therefore been made by means of model calculations.

The model calculations for the regional flow have been defined by using an analytical element model developed by STRACK (1976). The modeling has been performed over an area of about 25 km^2 where the following conditions are considered:

- Infiltration;
- Lakes with leaky bottom or given head;
- Creeks attributed to a given head;
- Cracks defined by their conductivity and width;
- The mine illustrated by a gallery;
- Properties of the fractured aquifer;
- Regional flow pattern outside the investigated area.

The model is used to generate flow paths and streamlines for the area as well as for close-ups in the immediate vicinity of the mine. Initial calculations show that the major flux takes place in the superficial rock mass, down to a depth of about 250 m. The present investigations are focused on depths of 300–1,200 m and to facilitate the modeling, only these deeper levels are considered.

The regional model is based on drainage patterns, fracture patterns, rock types and topography. The groundwater head amounts to about 300 m in the area NW of the modeled area. This gives a head distribution from 60 m (being the level of Lake Rosvalen adjacent to Stripa Mine), up to 300 m in NW. The geology of the area is dominated by supracrustal formation with only small plutonic bodies of granite. However, it should be noted that the extension of the granite is underestimated as the granitic volume increases with depth.

The calibration of the model was against known heads in the assumed unaffected rock mass. A modeling of the area produces a head distribution which fairly well agrees with potentials given by lakes and creeks in the area. The groundwater recharge to the deep levels amounts only to some 0.1 mm/year to be compared to the recharge at surface which may be in the order of 50–60 mm/year. Lakes and streams adjacent to the mine reduce the draining effect of the mine.

Two profiles are produced within the models, one starting in the NW part and passing through the mining area, and one from NNW through the mine. The existing streams affect the potential distribution and tend to extract water from the aquifer. However, in the vicinity of the mine, its drainage effect becomes strong and the water flow passes underneath the streams. In addition, some streams obtain a changed effect, *i.e.* influent streams become effluent.

Rough estimates of the transport times for the longer trajectories give a residence time of some 10,000 years. At least 70–80% of this residence time is in the supracrustal formation and only 20–30% in the granite. However, this estimate is based on a number of assumptions which make it highly uncertain.

GALE *et al.* (1987) have evaluated all of the Stripa hydraulic data from the SAC program and Phases I and II along with additional lab measurements to develop a three-dimensional flow model. Their interpretation indicates mine inflows perturb the flow regime to at least 3,000 m depth, and an average travel time of 600 years, from recharge to the underground mine. Such discrepancies can be expected in a highly heterogenous fractured rock medium where most data exist only in a very localized volume of the regional flow field. Unfortunately, proper characterization of the flow field was not an objective of the program.

Dewatering of the granite

The pressure sink made up by the mine has significantly affected the groundwater conditions in the granite. Over the years a continuous water inflow has taken place and as the

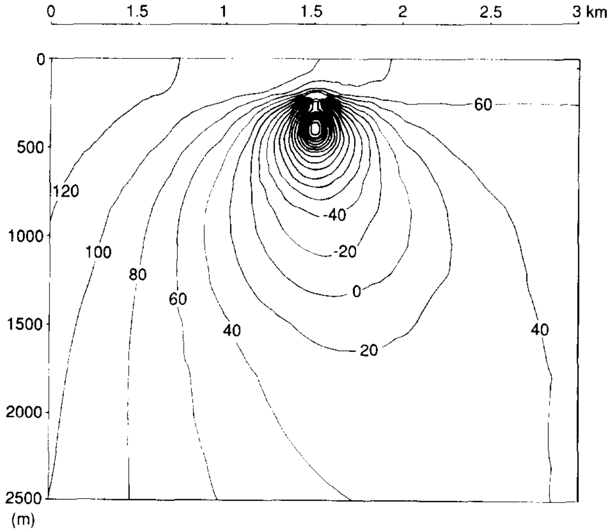

FIG. 10. Distribution of groundwater head around the mine from model calculations using case B in Fig. 8 and a finite element method.

Table 8. Total discharge in the boreholes since the drilling of the holes till the end of 1984.

Borehole	Total discharge m^3
N1	570
E1	480
V1	15.516
V2	3.020

mine was sunk, the drainage threshold was lowered. After the mining, only minor impacts on the groundwater system were introduced, and then mainly from different boreholes which also acted as drainage structures in the rock mass.

The total discharge from the mine amounted to about 470 l/min as an average value for the period January 1983 to December 1984. This discharge gives a total volume of water from the mine since the start of the SAC program to the end of 1988 of almost 250 m^3. In addition, the boreholes made for the present program have high discharges, especially boreholes V2 and V1. In Table 8, the total estimated discharge from the main boreholes are summarized. The values given represent the total discharge since the drilling of the boreholes till the end of 1984. The figures are based on the recorded discharge in relation to the borehole history, and are therefore only rough estimates. In total, the errors on the given figures are in the range of 10 percent.

The total effect from the drainage on the groundwater system is a shorter residence time. The recharge from the surface is more quickly flowing down to deeper levels in the rock mass, *i.e.* those levels which are of interest for water sampling and analysis. Also the groundwater flow from adjacent areas is faster which leads to a more complex mixing of different groundwaters. These conditions are of great significance for the interpretation of the hydrogeochemical data; a foreign groundwater may be sampled in the granite.

CONCLUDING REMARKS

The International Stripa Project has maintained a deep underground facility for research on high-level nuclear waste disposal. One of the unique features of the Stripa research is the detailed information on groundwater chemistry and associated rock and mineral chemistry in a Precambrian granitic terrain. The results of numerous chemical and isotopic determinations on rock, water and gas samples have led to new interpretations and new concepts for granite-water interactions at depths to 1 kilometer. They demonstrate the geochemical complexities that must be considered when modeling geochemical processes in crystalline rock and when attempting to integrate chemical processes with physical processes for groundwater flow in fractured media. New concepts have developed from this project that not only affect the overall safety assessment of crystalline rocks for radioactive waste disposal but also affect our scientific understanding of the subsurface and offer a new framework for future research.

Acknowledgements—We are grateful to SKB, especially Lars-Bertil Nielsen and Per-Erik Ahlstrom, and the Stripa Project managers, Hans Carlsson and Bengt Stillborg for all their support, encouragement and patience. Henrik Norlander and Daniel Lindstrom provided valuable field support. Numerous Swedish, American and European friends and colleagues all contributed to make this program work and the support of several institutions including the U.S.G.S., the University of Waterloo, the University of Paris (South), the University of Bath, the University of Arizona, I.A.E.A., the University of Bern, GSF, Stockholm University and CNRS at Strasbourg was essential.

Editorial handling: E. J. Reardon

REFERENCES

BARKER F. (1981) Introduction to special issue on granites and rhyolites: A commentary for the non-specialist. *J. Geophys. Res.* **86,** 10131–10135.

CARLSSON A. (1979) Characteristic features of a superficial rock mass in southern central Sweden. Horizontal and subhorizontal fractures and filling material. *Striae* **11,** 79.

CARLSSON L. and OLSSON T. (1985) Hydrogeological and hydrogeochemical investigations in boreholes. *Final Report, Stripa Project Tech. Rept. 85-10.*

CARLSSON L., OLSSON T. and STEJSKAL V. (1981) Core-logs of borehole V1 down to 505 m. *Stripa Project Tech. Rept. 81-05,* 28p.

CARLSSON L., OLSSON T. and STEJSKAL V. (1982a) Core-logs of the subhorizontal boreholes N1 and E1. *Stripa Project Tech. Rept. 82-04,* 44p.

CARLSSON L., EGERTH T., OLSSON T. and WESTLUND B. (1982b) Core-logs of the vertical hole V2. *Stripa Project Tech. Rept. 82-05,* 40p.

FRITZ B., CLAUER N. and KAM M. (1987) Strontium isotopic data and geochemical calculations as indicators for the origin of saline waters in crystalline rocks. In *Saline Water and Gases in Crystalline Rocks* (eds. P. FRITZ and S. K. FRAPE); *Geol. Assoc. Canada Spec. Paper 33,* pp. 121–126.

FRITZ P. and FRAPE S. K., eds. (1987) *Saline Water and Gases in Crystalline Rocks, Geol. Assoc. Canada Spec. Paper 33,* 259p.

FRITZ P., BARKER J. F. and GALE J. E. (1980) Summary of geochemical activities at the Stripa test site during FY1979/80. *Waterloo Res. Inst. Rept. 803-12.*

GALE J. (1982) Hydrogeological characteristics of the Stripa site. *University of Waterloo Rept. 003C.*

GALE J., MACLEOD R., WELHAN J., COLE C. and VAIL L. (1987) Hydrogeological characterization of the Stripa site. *Stripa Tech. Rept. 87-15,* 146p.

GEIJER P. (1938) Stripa odalsfalte geologi. *Swedish Geological Survey Rept., Ser. Ca-28.*

HEIER K. F. and ROGERS J. J. W. (1963) Radiometric determinations of thorium, uranium and potassium in basalts and in two magmatic differentiation series. *Geochim. Cosmochim. Acta* **27,** 137–154.

KOARK H. J. and LUNDSTRÖM I. (1979) Berggrundskartan Lindesberg SV. *Swedish Geological Survey, Ser. Af-126.*

LUNDSTROM L. and STILLE H. (1978) Large scale permeability test of granite in the stripa mine and thermal conductivity test. *SAC Rept.-02, LBL-7052,* 33p.

NORDSTROM D. K., LINDBLOM S., DONAHOE R. J. and BARTON C. C. (1989) Fluid inclusions in the Stripa granite and their possible influence on the groundwater chemistry. *Geochim. Cosmochim. Acta* **53,** 1741–1755 (this issue).

NORTON D. and KNAPP R. (1977) Transport phenomena in hydrothermal systems: The nature of porosity. *Amer. J. Sci.* **277,** 913–936.

PARSON M. L. (1972) Determination of hydrogeological properties of fissured rocks, *24th Intl. Geol. Congr.* **11,** 89–99.

PAULSRYD B. (1941) *Ore Mapping in the Stripa Mine.* Stallbergs Grufe AB.

STRACK O. D. L. (1976) A single-potential solution for regional interface problems in coastal aquifers. *Water Resour. Res.* **12,** 1165–1174.

WELIN E. (1964) Pitchblende-bearing vein fillings in the Stripa and Blanka iron ores. *Trans. Geol. Soc. Sweden* **86,** 215–270.

WITHERSPOON P. A., COOK N. G. and GALE J. (1980) Progress with field investigations at Stripa. *SAC Rept. -27, LBL-10559,* 50p.

WOLLENBERG H., FLEXSER S. and ANDERSSON L. (1980) Petrology and radiogeology of the Stripa pluton. *LBL-11654.*